solids

MDPI

Article

Optical and Amplified Spontaneous Emission Properties of 4H-Pyran-4-Ylidene-2-Cyanoacetate Fragment Containing 2-Cyanoacetic Acid Derivative in PVK, PSU, or PS Matrix

Patricija Paulsone [1], Julija Pervenecka [1], Elmars Zarins [2], Valdis Kokars [2] and Aivars Vembris [1,*]

[1] Institute of Solid State Physics, University of Latvia, 8 Kengaraga Str., LV-1063 Riga, Latvia
[2] Faculty of Natural Sciences and Technology, Riga Technical University, 3/7 Paul Walden Str., LV-1048 Riga, Latvia; valdis.kokars@rtu.lv (V.K.)
* Correspondence: aivars.vembris@cfi.lu.lv

Abstract: Organic solid-state lasers are highly promising devices known for their low-cost fabrication processes and compact sizes and the tunability of their emission spectrum. These lasers are in high demand across various industries including biomedicine, sensors, communications, spectroscopy, and military applications. A key requirement for light-emitting materials used in a light-amplifying medium is a low threshold value of the excitation energy of the amplified spontaneous emission (ASE). A newly synthesized non-symmetric red-light-emitting laser dye, Ethyl 2-(2-(4-(bis(2-(trityloxy)ethyl)amino)styryl)-6-tert butyl-4H-pyran-4-ylidene)-2-cyanoacetate (KTB), has shown great promise in meeting this requirement. KTB, with its attached bulky trityloxyethyl groups, has the ability to form amorphous thin films from a solution using a wet-casting method. Recent experiments have demonstrated that KTB exhibits a low ASE threshold value. This study focused on investigating the optical and amplified spontaneous emission properties of KTB in poly(N-vinylcarbazole) (PVK), polysulfone (PSU), and polystyrene (PS) matrices at various concentrations. The results showed that as the concentration of the dye increased, a redshift of the photoluminescence and ASE spectra occurred due to the solid-state solvation effect. The lowest ASE threshold value of 9 μJ/cm^2 was achieved with a 20 wt% concentration of KTB in a PVK matrix, making it one of the lowest excitation threshold energies reported to date.

Keywords: cyanoacetic acid derivative; molecular glass; amorphous materials; amplified spontaneous emission; organic laser dyes; guest–host system

Citation: Paulsone, P.; Pervenecka, J.; Zarins, E.; Kokars, V.; Vembris, A. Optical and Amplified Spontaneous Emission Properties of 4H-Pyran-4-Ylidene-2-Cyanoacetate Fragment Containing 2-Cyanoacetic Acid Derivative in PVK, PSU, or PS Matrix. *Solids* **2024**, *5*, 520–532. https://doi.org/10.3390/solids5040035

Academic Editor: Mirosław Mączka

Received: 28 August 2024
Revised: 15 October 2024
Accepted: 17 October 2024
Published: 19 October 2024

1. Introduction

Organic materials play a crucial role in the advancement of electronics and photonics due to their unique properties such as flexibility, light weight, and low-cost production. In particular, organic semiconductors offer promising opportunities for high-performance devices in optoelectronics applications [1–3]. The development of solid-state lasers utilizing organic materials is still an active field of research, with ongoing efforts focused on enhancing their efficiency, reliability, and tunability. These lasers utilize non-crystalline structure films composed of organic compounds, allowing for a wide range of applications [4–6]. Organic molecules serve as emitters within the laser-active medium, contributing to the efficiency and effectiveness of the laser system [5,7].

The deposition of thin films from a solution of organic light-emitting materials has made organic solid-state lasers a competitive alternative to the more expensive traditional inorganic lasers. The key advantages of organic solid-state lasers include cost-effective fabrication processes, compact sizes, and seamless integration into photonic devices. These features have opened up new technological possibilities for organic solid-state lasers in various fields such as spectroscopy [8], communication [9], sensors [10–12], and biochips [13,14].

Until now, organic emitters have been able to cover a spectral range from blue to infrared [15–18]. The excitation threshold energy for amplified spontaneous emission (ASE) depends on the emitted wavelength, with the lowest values for neat amplification media ranging between 0.7 and 50 $\mu J/cm^2$ [15,19–21]. All mentioned values were obtained with a nanosecond excitation pulse length. However, achieving even lower excitation threshold values for ASE in neat thin films of light-emitting materials has been challenging due to the many intermolecular interactions between dye molecules. This interaction leads to luminescence quenching, reducing the photoluminescence quantum yield (PLQY) and increasing the ASE excitation threshold energy.

To overcome these challenges, increasing the distance between dye molecules is crucial. This can be achieved through two methods: increasing the spatial size of the molecule by creating a dendrimer-like structure or utilizing a host–guest system, where laser dyes are separated by another material matrix, such as Alq_3 [22]. The best ASE threshold energy for guest–host systems has been achieved between 0.1 and 10 $\mu J/cm^2$ [23–26], which is at least one order of magnitude lower than that of neat thin films. A polymer matrix is an alternative host, in which laser dyes are dispersed to reduce intermolecular interaction. Polymethylmethacrylate or polystyrene has been used as a matrix [27–29]. However, for planar and rigid molecules, the polymer matrix is only effective for low-concentration samples, as demonstrated with perylenediimide dyes. This is due to the strong interaction between molecules, which decreases the photoluminescence (PL) and amplified spontaneous emission (ASE) properties as the molecule concentration increases. By attaching diphenylphenol to the perylenediimide dye to make it more bulky, the PL and ASE properties can be improved at higher dye concentrations [30].

In the past, we have enhanced the ASE properties of the popular laser dye DCM [31], which has demonstrated notable light-emitting characteristics. To address the high intermolecular interaction between DCM molecules, we introduced bulky groups at the electron donor portion [32,33]. This modification enabled the creation of neat thin films from a solution, resulting in an achieved ASE threshold energy of 95 $\mu J/cm^2$.

We have recently reported the synthesis of a new glass-forming derivative of 2-cyanoacetic acid, known as ethyl 2-(2-(4-(bis(2-(trityloxy)ethyl)amino)styryl)-6-tert-butyl-4H-pyran-4-ylidene)-2 cyanoacetate (KTB). This compound exhibited a high photoluminescence quantum yield (PLQY) of 23% and a low excitation threshold energy of amplified spontaneous emission (ASE) of 24 $\mu J/cm^2$ in a neat thin film [33], making it one of the most efficient materials to date in terms of ASE excitation threshold value. By incorporating KTB molecules into a polymer matrix, we can enhance the emission properties of the system by increasing the PLQY and reducing the ASE excitation threshold energy.

In this study, we investigated the optical and ASE properties of the original non-symmetric 2-cyanoacetic acid derivative, KTB, at various concentrations in poly(N-vinylcarbazole) (PVK), polysulfone (PSU), and polystyrene (PS) matrices. These polymers were chosen for their high refractive indices (PVK: 1.696; PSU: 1.642; PS: 1.593), which are essential for efficient planar waveguide preparation. We prepared and analyzed three types of guest–host systems with KTB concentrations ranging from 1% to 70% in PVK, PSU, and PS. The neat thin film of KTB molecules served as the reference material for comparison.

2. Materials and Methods

2.1. Investigated Organic Compound

Ethyl 2-(2-(4-(bis(2-(trityloxy)ethyl)amino)styryl)-6-tert-butyl-4H-pyran-4-ylidene)-2-cyanoacetate (KTB) is a novel non-symmetric red, near-infrared light-emitting dye, as depicted in Figure 1. This molecule comprises a 4-substituted-4H-pyran as an electron acceptor and an electron donor group with two bulky trityloxyethyl groups attached at the donor side. The presence of these bulky trityloxyethyl groups serves to weaken intermolecular interactions, thereby reducing crystallization and facilitating the preparation of amorphous thin films from the solution. KTB demonstrates excellent solubility in

chloroform and dichloromethane. For a comprehensive synthesis of KTB, please refer to the detailed description provided elsewhere [33].

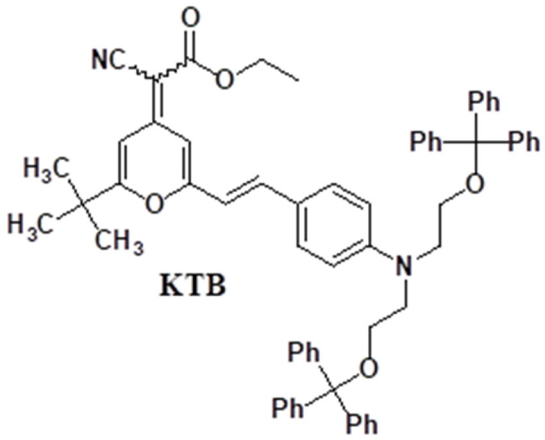

Figure 1. Chemical structure of KTB.

2.2. Sample Preparation for Optical Characterization

Three distinct types of guest–host systems were created for this study. Initially, KTB was dissolved in dichloromethane. The volume ratio of organic compound mass to solvent was kept constant at 30 mg/mL, and the appropriate amount of the prepared KTB–dichloromethane solution was added to PVK (Sigma Aldrich, St. Louis, MO, USA, No. 368350), PSU (Sigma Aldrich No. 428302), and PS (Sigma Aldrich No. 430102). By varying the concentration ratios of the host polymers and guest dyes in the system, three series of samples were produced with KTB concentrations of 1, 5, 10, 20, 30, 50, and 70 wt%.

A neat thin film was prepared according to the method described in reference [33]. The consistent volume ratio of organic compound to solvent ensured uniform film thickness across all samples. Prior to film deposition, all glass substrates were cleaned with dichloromethane and heated at 115 °C for 15 min to enhance the adhesion between the solution and substrate. The solutions were spin-coated onto the substrates for 40 s at a spin speed of 800 rpm and acceleration of 800 rpm/s, followed by drying at 85 °C for 10 min. The thickness of the films, measured using the Surface Profile Measuring System Veeco Dektak 150 (Bruker, Karlsruhe, Germany), ranged between 300 and 400 nm, meeting the optical waveguide conditions for the amplified spontaneous emission wavelength between 620 nm and 640 nm (see Figure 2). Due to the decreases in refractive index in the order of PVK (1.696), PSU (1.642), and PS (1.593), an effective refractive index decrease also occurred, inducing a smaller guidance effect due to more evanescent light appearing through the glass (see Figure 2).

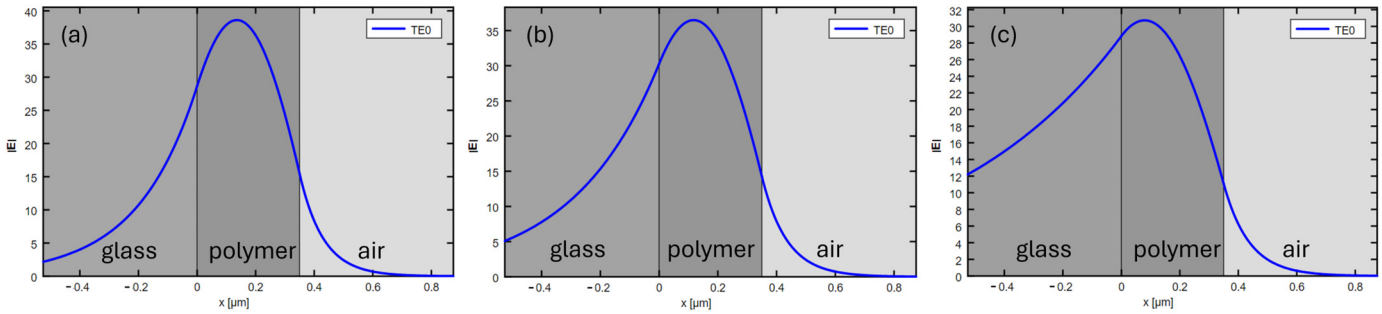

Figure 2. Light confinement in the planar waveguide for (**a**) PVK, (**b**) PSU, and (**c**) PS. Calculations were conducted in the OMS program.

2.3. Measurement Systems

The absorption spectra of the thin films were analyzed using a Cary 7000 Universal Measurement Spectrophotometer (Agilent, Santa Clara, CA, USA). The photoluminescence spectra and photoluminescence quantum yield were measured using the calibrated system Fluorescence spectrometer Pico Master 1 (PicoQuant GmbH, Berlin, Germany). All samples were excited at the maximum KTB absorption wavelength of 471 nm for photoluminescence, photoluminescence quantum yield, and amplified spontaneous emission (ASE). ASE was excited by an Ekspla 310 series pulse laser (Ekspla, Vilnius, Lithuania) with a tunable wavelength, featuring a pulse duration of 10 ns and a repetition rate of 10 Hz. The measurements were conducted using a self-made system that utilized a variable line technique, focusing on a 3 mm long and 0.4 mm wide line on the sample surface. The experimental scheme and set-up for ASE and PLQY are detailed in publication [34].

Optical images of the thin films' morphology were captured using a high-resolution optical microscope in transmission mode, the Nikon ECLIPSE L150 (Nikon Instruments Inc., Melville, NY, USA). The roughness of the films was assessed using a profilometer, the Dektak 150 Surface Profiler (Bruker, Karlsruhe, Germany).

3. Results and Discussion

3.1. Optical Images

The morphologies of the KTB:PVK, KTB:PS, and KTB:PSU guest–host system films at varying dye concentrations were examined using high-resolution optical images (see Figure 3) and surface profiles. The morphology of the films exhibited significant variations depending on the polymer and dye concentrations utilized. The most notable structural inhomogeneities were observed in samples with low (1–20 wt%) concentrations of laser dyes (see Figure 3a–c), which disappeared at higher concentrations (see Figure 3d–f). Two types of inhomogeneities can be observed. Small clusters, appearing as light dots, can be observed at both 20% and 70% concentrations, but are larger in the 20% samples, being of the first type. Changes in the thickness of the thin film, which can be seen as lighter and darker areas in 20% of the samples, are the second type. Both may have the same origin and are related to the complex process of solid formation due to the different possible orientations of the polymer molecular chains. The pronounced structural differences were particularly evident in the KTB:PSU and KTB:PS samples. The surface roughness decreased with increasing dye concentrations in the system, ranging from approximately 40 nm for 1 wt% samples to 7–5 nm for the 70 wt% samples and 3 nm for the 100 wt% samples. This observation clearly indicates that the islands and stripes present are a result of long polymer molecular chains. While the polymer chain orientation due to centrifugal forces may play a role, no correlation between the film roughness and polymer molecular weight was identified. The specific interaction between polymer chains, particularly notable in PSU and PS, is likely the origin of these structures.

The KTB:PVK samples exhibit a superior quality of the layer surface and a well-controlled, expected thickness of the film. Upon closer examination in all-optical images, small transparent dots resembling bubbles can be identified. A more thorough analysis of the structure and properties, such as polarity, dielectric constant, and glass transition temperature, of the polymers used suggests that these dots are agglomerations of KTB. The exceptional quality of the KTB:PVK films can be attributed to the high polarity and density of PVK. The former facilitates the solvation of the KTB, while the latter contributes to the formation of smooth film surfaces. Conversely, the roughness and inferior optical quality of the PS thin films can be linked to the lower polarity and density of PS, resulting in the poor solvation of KTB. Furthermore, the formation of shiny dots is influenced by the disparate glass transition temperatures of KTB and the polymers. The high glass transition temperatures of PVK and PS, combined with the drying temperature used for the samples, create a non-eutectic system that leads to the formation of glass-formed areas in the film—the shiny dots. As the concentration of dye increases, the shiny dots on optical

images become less discernible, likely due to the formation of larger glass-formed areas with a higher density of KTB.

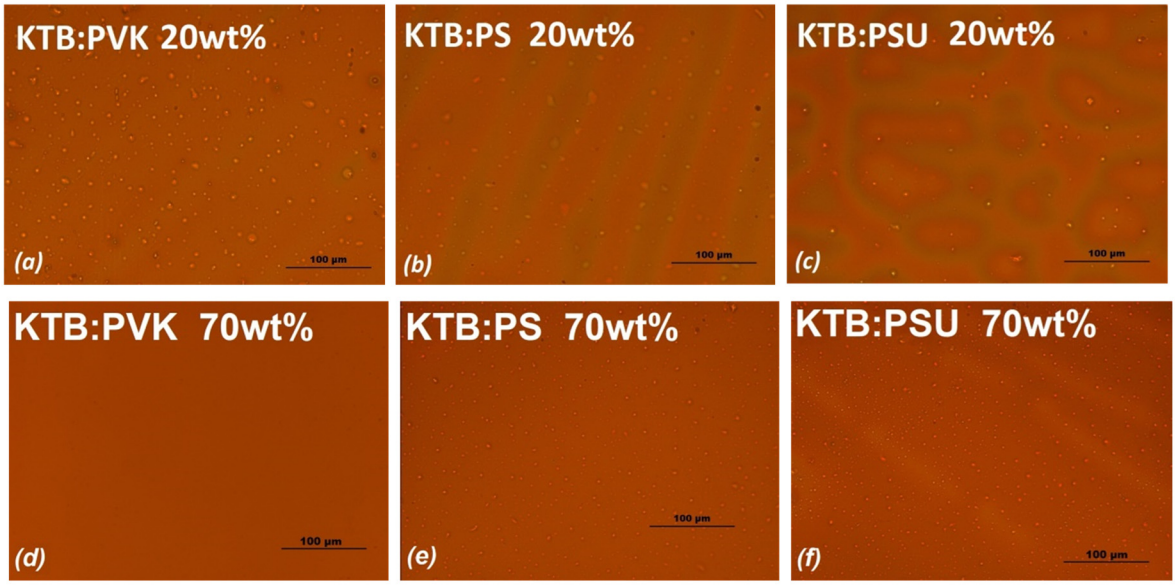

Figure 3. High-resolution optical images of the samples' surface morphologies. The sample composition and organic compound concentration in polymer is shown in each subfigure. Optical images were obtained at ×200 magnification.

3.2. Optical Properties

The normalized absorption spectrum of the pure KTB sample and samples containing 20 wt% of KTB in PVK, PSU, PS matrices are depicted in Figure 4. The maximum absorption bands are typically around 471 nm, with slight variations of up to 10 nm depending on the host polymer. The shapes of these spectra exhibit similarities, with slight broadening observed as the dielectric constant of the polymer increases from PS to PVK. These changes in the maximum absorption position and spectral broadening can be attributed to the solvation of KTB within the polymer matrix, influenced by the varying dielectric constants of the solid solution systems. This leads to the reorganization of solvent and solute molecules into solid solvation complexes, resulting in alterations in the stabilization of the dye molecules' ground and first excited states, manifesting as shifts in the shape and intensity of certain bands in the absorption spectrum [35].

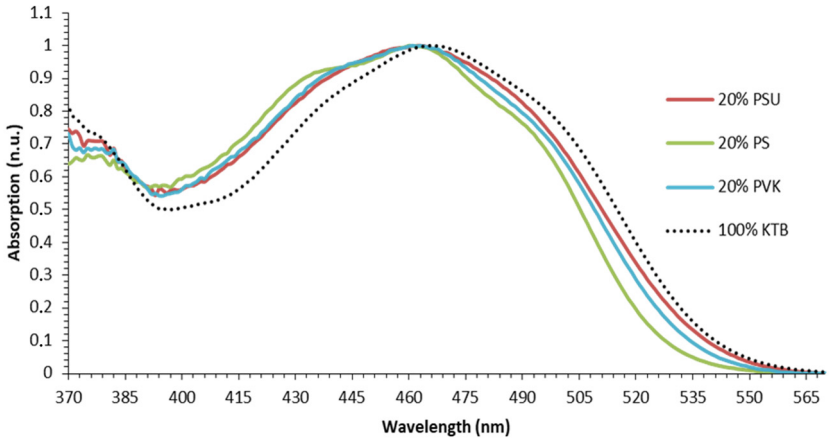

Figure 4. Absorption spectra of thin films of 20 wt% of investigated compound in different matrices. Absorption spectrum for neat KTB thin film is given for comparison.

In the case of pure KTB, its optical properties are primarily influenced by the 2-cyanoacetate electron-withdrawing fragment, with increased light absorption observed in the 460–480 nm range, attributed to the electron donor bulky trityloxyethyl group. The less pronounced absorption band from 480 to 495 nm is contributed by the -CN group [33]. The bulky trityloxyethyl and tert-butyl groups have a minimal impact on the electron transitions within the molecule [34].

Irrespective of the host polymer used or the weight ratios of compounds within the system, the photoluminescence spectra of all the investigated host–guest systems exhibit similar shapes. The small variations in the PL spectrum can be attributed to the different dielectric constant of the polymer (see Figure 5a). However, the maximum position of the PL spectra is heavily influenced by the weight ratios of KTB in the host. A noticeable redshift in the PL spectra was observed with an increase in KTB dye concentration in all investigated host–guest systems (see Figure 5b). This shift in the PL spectra, typically uncommon in solid-state materials, is more commonly observed in solutions and is known as the solvatochromic effect. This effect allows for the tuning of the photoluminescence spectra of specific compounds by using solvents with varying polarities (dielectric constants). Since KTB dye molecules are dissolved in a polymer matrix, the investigated host–guest systems can be considered solid solutions, where the solvatochromic effect can also occur. In solids, this phenomenon is referred to as the solid-state solvation effect, which is attributed to changes in the system's dielectric constant, resulting from fluctuations in the volume fraction of the investigated dye in the host–guest system [34,36–38]. Similar effects have been observed previously in different host–guest systems involving pyranyliden derivatives and 2-cyanoacetic acid derivatives [36].

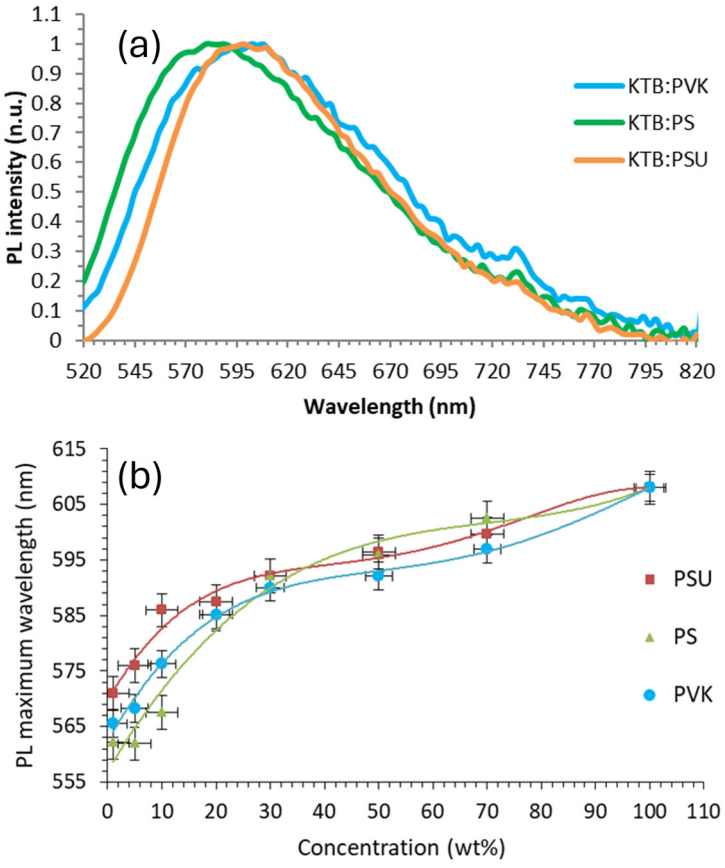

Figure 5. (**a**) Photoluminescence spectra of 20 wt% KTB compound in different polymers. (**b**) Wavelength of photoluminescence maximum at different KTB concentrations.

In all host–guest systems investigated, the increase in KTB concentration results in a decrease in the photoluminescence quantum yield (PLQY), as shown in Figure 6. This decrease is attributed to the heightened intermolecular interaction between KTB molecules, which occurs as the distance between chromophore molecules decreases. At low concentrations (<5 wt%), the KTB:PSU system exhibits the highest PLQY at 56%. The PLQYs of the KTB:PS and KTB:PVK systems at low concentrations are comparable, at 40% and 43%, respectively. Across all weight ratios, the KTB:PSU system consistently demonstrates the highest PLQY, surpassing those of the KTB:PS and KTB:PVK systems by a factor of 1/3 or more. The varying patterns of PLQY decreases in systems at higher concentrations may be attributed to differences in the length and structure of the polymer chains. For instance, in systems with longer molecular chains (such as PSU), the reduction in distance between chromophore molecules is not as pronounced, even at high KTB concentrations, unlike in PVK and PS systems. This suggests that a PSU polymer mitigates the interaction between KTB molecules, thereby reducing photoluminescence quenching and resulting in higher PLQYs in the KTB:PSU systems. Even at very high concentrations (70 wt%) of KTB, the PLQY of the KTB:PSU system exceeds that of pure KTB by a factor of 1/3.

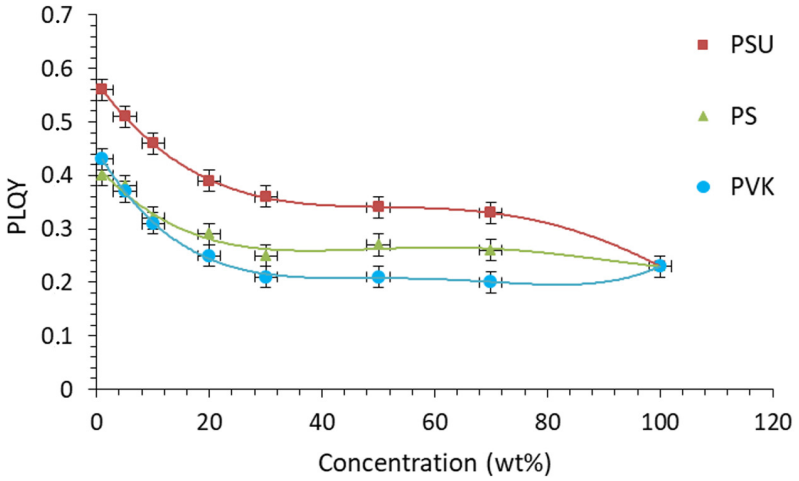

Figure 6. Dependence of photoluminescence quantum yield on the laser dye concentration in PVK, PS, and PSU matrices.

3.3. Amplified Spontaneous Emission

To induce amplified spontaneous emission (ASE) in all thin films, a wavelength of 471 nm, corresponding to the pure KTB absorption maximum, was utilized. The presence of ASE in the studied systems was identified by the emergence of a narrow, highly intense peak atop the photoluminescence band (see Figure 7a–c). The full width at half maximum (FWHM) of the ASE peak (photoluminescence part is included) exhibited an inverse relationship with the energy of the pump beam, with the FWHM decreasing by approximately one order of magnitude as the pump beam energy increased. In all investigated host–guest systems with KTB concentrations below 5 wt%, ASE could not be stimulated even at excitation energies exceeding 2 mJ/cm^2 despite having the highest PLQY. This phenomenon can be attributed to the critical concentration of the molecule that is required to sustain a consistent stimulated emission. When the concentration is too low, the necessary level of excited molecules is not achieved, resulting in insufficient amplification of the spontaneously emitted light, which cannot be rectified by a higher PLQY. Conversely, at a higher concentration, such as 5 wt%, the molecular density is five times larger, while the PLQY decreases by 20%. Ultimately, it should give a sufficient number of emitting species to be able to generate ASE. The maximum positions of the ASE peaks were slightly redshifted in comparison to the maximum positions of the PL emission spectra. This shift is attributed to the theoretical assertion that the effective cross-section of

stimulated emission should be greater on the higher-energy side of the PL spectral band maximum [32]. Equation (1) provides a relationship that can be used to determine the position of the amplified spontaneous emission peak [39]:

$$\sigma_{em}(\lambda) \propto F(\lambda) \cdot \lambda^4, \quad (1)$$

where $\sigma_{em}(\lambda)$ is the stimulated emission cross-section, $F(\lambda)$ is the fluorescence quantum distribution function, and λ is the light wavelength.

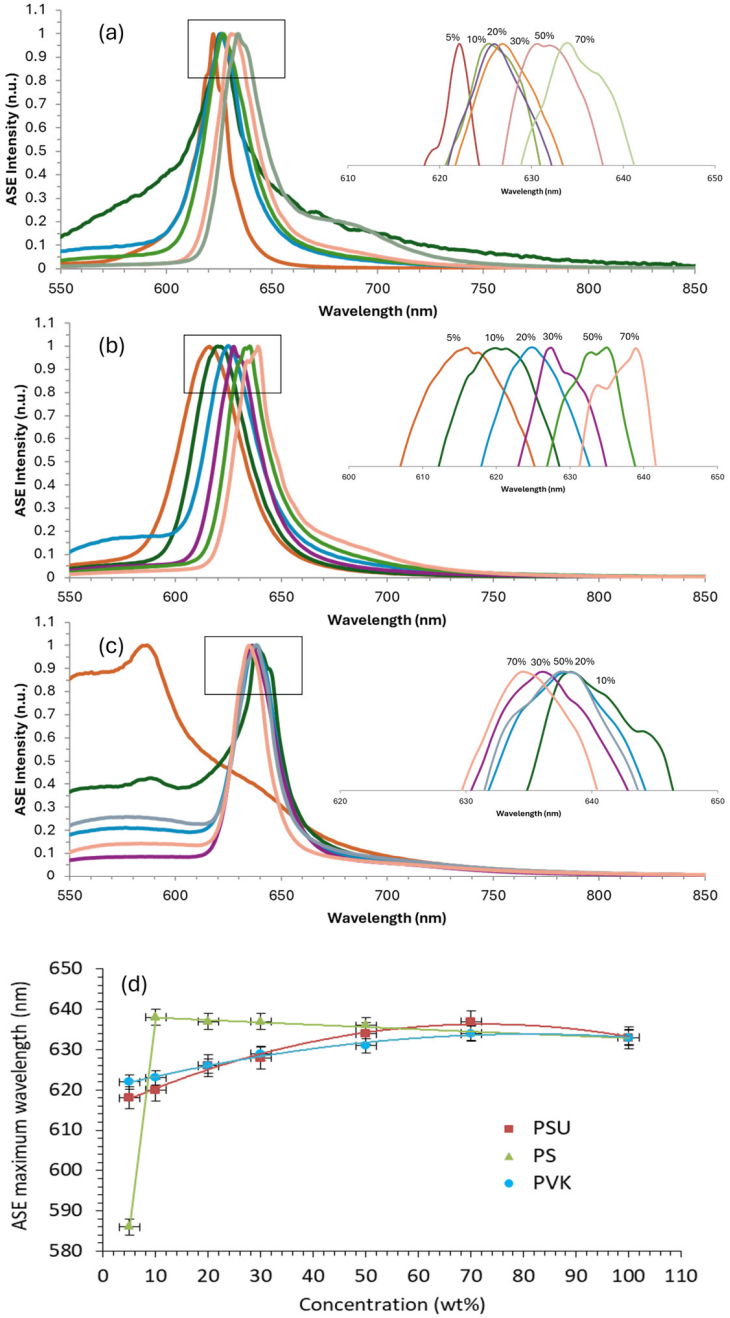

Figure 7. Amplified spontaneous emission spectra at different dye concentrations in the (**a**) PVK, (**b**) PSU, and (**c**) PS matrices. (**d**) Dependence of ASE maximum wavelength on dye concentration.

Similar to photoluminescence, less pronounced redshifts of ASE spectra were observed with an increase in the concentration of dye molecules in the polymer matrix (see Figure 7a–c). The redshift in the ASE spectra is attributed to the solid-state solvation ef-

fect [34,36–38]. However, these changes are not as prominent due to the overlapping of the PL and absorption spectral bands. According to this theory, the peak of amplified spontaneous emission can only be formed in parts of the photoluminescence spectral band where the optical loss coefficient is smaller than the optical gain [32]. This implies that stimulated emission will occur in the spectral emission region, where the difference between the loss and gain coefficients is greater than zero, meaning that the difference between the stimulated emission and absorption cross-section is positive. The amplification coefficient can be described by the following equation:

$$P(\lambda) = ((\sigma_{em}(\lambda) - \sigma^*(\lambda))n^* - \sigma(\lambda)\cdot(N - n^*)), \quad (2)$$

where n^* is the density of excited molecules; N is the total density of molecules; and $\sigma(\lambda)$, $\sigma_{em}(\lambda)$, and $\sigma^*(\lambda)$ are cross-sections of the ground state absorption, stimulated emission, and excited state absorption, respectively.

In all investigated guest–host systems, the absorption and photoluminescence (PL) spectra overlap on the left side (small wavelength) of the photoluminescence band. The photoluminescence spectra demonstrate a solid-state solvation effect, while the absorption spectra remain unchanged with concentration. It is observed that there is a larger overlap between the PL and absorption spectra in samples with low laser dye concentrations. If we consider that the origin of the amplified spontaneous emission (ASE) is the same electron transition in the molecule for all concentration samples, then absorption will have a greater impact on the spectral position of the ASE in low-concentration samples, shifting it towards the red spectral region. In conclusion, the redshift of the ASE is influenced by both absorption and the solid-state solvation effect.

Amplified spontaneous emission is blueshifted in low-concentration samples (5% and 10%) with PS as the polymer. It is more likely to be associated with the 0-0 transition, while at higher concentrations, it is more likely to be the 0-1 or 0-2 transition. As has already been said before, as the concentration increases, the absorption increases directly in the region of small wavelength light, which means that the 0-0 or 0-1 transition is significantly extinguished and only higher-order transitions can emit [40].

The excitation threshold energy value for ASE decreases as the concentration of molecules in the polymer matrix increases, as shown in Figure 8. In the KTB:PVK and KTB:PS systems, the excitation threshold energy value decreases from 5 to 20 wt% (5–10 wt% in the case of KTB:PSU), reaching a minimum at 20 wt% (10 wt% for KTB:PSU), and then increases with the increasing concentration of dye molecules (see Figure 8 and Tables 1–3). The ASE excitation threshold energy was below 60 μJ/cm^2 for all dye concentrations in the KTB:PVK and KTB:PSU systems. However, the KTB:PS systems exhibited poorer ASE properties, with excitation threshold energy values that were significantly higher than 100 μJ/cm^2. This indicates that a lower threshold excitation energy for ASE can be achieved in host–guest systems with polymers that have high dielectric constants and refractive indices, leading to better waveguiding properties of the system (see Figure 2). A thicker waveguide also could be used to decrease the ASE excitation threshold energy value due to better light-guiding properties and higher absorption, but in this case, the experiments were carried out under similar conditions so that the results can be compared.

The ASE excitation threshold energy is determined from the emission intensity changes by inversing the excitation pulse energy (see the inset of Figure 8). A detailed description can be found in [32]. The lowest ASE excitation threshold energy value of 9 μJ/cm^2 was achieved in the KTB:PVK system at a 20 wt% concentration of dye molecules, while the lowest value of 16 μJ/cm^2 was reached in the KTB:PSU system at 10 wt%. These values are among the lowest for red-light-emitting laser dye systems.

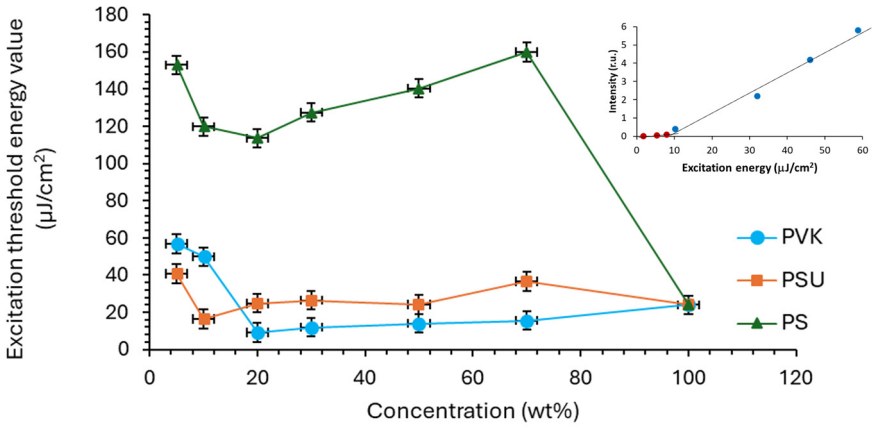

Figure 8. Amplified spontaneous emission excitation threshold energy at different KTB dye concentrations. Insert: determination of ASE threshold energy for 20 wt% of KTB in PVK matrix.

Table 1. Optical properties of thin films of KTB in PVK matrix at different concentrations.

Concentration, wt%	λ_{abs}, nm	λ_{PL}, nm	$FWHM_{PL}$, nm	PQLY, %	λ_{ASE}, nm	$FWHM_{ASE}$, nm	E_{th}, μJ/cm²
1	461 ± 2	566 ± 2	108 ± 1	43 ± 2	-	-	-
5	461 ± 2	568 ± 2	112 ± 2	37 ± 2	622 ± 2	17 ± 2	57 ± 6
10	461 ± 2	576 ± 2	112 ± 2	32 ± 2	623 ± 2	14 ± 2	50 ± 5
20	461 ± 2	585 ± 2	101 ± 2	25 ± 2	626 ± 2	22 ± 2	9 ± 1
30	461 ± 2	590 ± 2	116 ± 2	21 ± 2	629 ± 2	21 ± 2	12 ± 1
50	461 ± 2	592 ± 2	119 ± 2	21 ± 2	631 ± 2	22 ± 2	14 ± 1
70	461 ± 2	597 ± 2	114 ± 2	20 ± 2	634 ± 2	21 ± 2	16 ± 2

Table 2. Optical properties of thin films of KTB in PSU matrix at different concentrations.

Concentration, wt%	λ_{abs}, nm	λ_{PL}, nm	$FWHM_{PL}$, nm	PQLY, %	λ_{ASE}, nm	$FWHM_{ASE}$, nm	E_{th}, μJ/cm²
1	463 ± 2	571 ± 2	100 ± 1	56 ± 2	-	-	-
5	463 ± 2	576 ± 2	102 ± 2	51 ± 2	618 ± 2	33 ± 2	41 ± 4
10	463 ± 2	586 ± 2	107 ± 2	46 ± 2	620 ± 2	29 ± 2	16 ± 2
20	463 ± 2	588 ± 2	108 ± 2	39 ± 2	626 ± 2	24 ± 2	25 ± 2
30	463 ± 2	592 ± 2	105 ± 2	36 ± 2	628 ± 2	23 ± 2	26 ± 3
50	463 ± 2	596 ± 2	114 ± 2	34 ± 2	634 ± 2	19 ± 2	24 ± 2
70	463 ± 2	600 ± 2	115 ± 2	33 ± 2	637 ± 2	19 ± 2	37 ± 4

Table 3. Optical properties of thin films of KTB in PS matrix at different concentrations.

Concentration, wt%	λ_{abs}, nm	λ_{PL}, nm	$FWHM_{PL}$, nm	PQLY, %	λ_{ASE}, nm	$FWHM_{ASE}$, nm	E_{th}, μJ/cm²
1	460 ± 2	562 ± 2	101 ± 1	40 ± 2	-	-	-
5	460 ± 2	562 ± 2	105 ± 2	38 ± 2	586 ± 2	14 ± 2	153 ± 15
10	460 ± 2	568 ± 2	111 ± 2	32 ± 2	638 ± 2	17 ± 2	120 ± 12
20	460 ± 2	585 ± 2	129 ± 2	29 ± 2	637 ± 2	19 ± 2	114 ± 11
30	460 ± 2	592 ± 2	122 ± 2	25 ± 2	637 ± 2	21 ± 2	127 ± 13
50	460 ± 2	596 ± 2	128 ± 2	27 ± 2	636 ± 2	19 ± 2	140 ± 14
70	460 ± 2	603 ± 2	133 ± 2	26 ± 2	634 ± 2	17 ± 2	160 ± 16

λ_{abs}—wavelength of absorption maximum, λ_{PL}—wavelength of photoluminescence maximum, PLQY—photoluminescence quantum yield, λ_{ASE}—maximum wavelength of amplified spontaneous emission, FWHM—full width of half maximum of PL or amplified spontaneous emission band, E_{th}—irradiation threshold energy density at which amplified spontaneous emission appears. (KTB: λ_{abs}—471 nm, λ_{PL}—608 nm PLQY—23%, λ_{ASE}—633 nm, $FWHM_{PL}$—170 nm, $FWHM_{ASE}$—15 nm, E_{th}—24 μJ/cm² [33]).

4. Conclusions

The solid-state solvation effect is evident in the photoluminescence (PL) and amplified spontaneous emission (ASE) emission spectra of the KTB dye when mixed in a polymer matrix. This effect allows for the tuning of the KTB emission spectra by adjusting its concentration in the host–guest system. The tuning range can reach up to 11 nm for KTB:PVK and 15 nm for KTB:PSU. The highest photoluminescence quantum yield (PLQY) is observed in the KTB:PSU samples, while the second-lowest ASE excitation threshold energy value of 16 $\mu J/cm^2$ is found in the 10 wt% system. Interestingly, the lowest ASE excitation energy of 9 $\mu J/cm^2$ is recorded in the 20 wt% KTB:PVK sample, despite having the lowest PLQY. This discrepancy between the lowest ASE excitation threshold energy and maximum PLQY can be attributed to the high refractive index of the polymer in the KTB:PVK system, which enhances the waveguide quality. Therefore, both the PLQY and refractive index of the host material must be considered when evaluating ASE properties and fabricating the organic solid-state laser. The thickness of the waveguide could also impact the ASE properties; therefore, samples with similar thicknesses were compared. The ASE excitation threshold energy obtained in this study is among the lowest for red emitters compared to previously investigated chromophores. Both the KTB:PVK and KTB:PSU systems show promise for light amplification. However, when considering the fabrication of an organic solid-state laser-active medium, the KTB:PVK system appears more favorable due to the higher refractive index of the polymer.

In conclusion, the solid-state solvation effect in the KTB dye mixed with a polymer matrix offers a unique opportunity for tuning emission spectra and enhancing ASE properties. The findings of this study contribute to the development of efficient and promising systems for organic solid-state lasers.

Author Contributions: Conceptualization, A.V. and P.P.; methodology, P.P., J.P. and E.Z.; formal analysis, P.P., J.P. and E.Z.; investigation, P.P., J.P. and E.Z.; writing—original draft preparation, P.P.; writing—review and editing, A.V. and V.K.; visualization, P.P.; supervision, A.V. and V.K.; funding acquisition, A.V. All authors have read and agreed to the published version of the manuscript.

Funding: European Regional Development Fund (ERDF) 1.1.1.1 Activity Project Nr. 1.1.1.1/16/A/046 "Application assessment of novel organic materials by prototyping of photonic devices".

Data Availability Statement: The data presented in this study are available on request from the corresponding author.

Conflicts of Interest: The authors declare no conflict of interest.

References

1. Solak, E.K.; Irmak, E. Advances in Organic Photovoltaic Cells: A Comprehensive Review of Materials, Tech-nologies, and Performance. *RSC Adv.* **2023**, *13*, 12244–12269. [CrossRef] [PubMed]
2. Nawaz, A.; Merces, L.; Ferro, L.M.M.; Sonar, P.; Bufon, C.C.B. Impact of Planar and Vertical Organic Field-Effect Transistors on Flexible Electronics. *Adv. Mater.* **2023**, *35*, 220480. [CrossRef] [PubMed]
3. Nayak, D.; Choudhary, R.B. A Survey of the Structure, Fabrication, and Characterization of Advanced Organic Light Emitting Diodes. *Microelectron. Reliab.* **2023**, *144*, 114959. [CrossRef]
4. Samuel, I.D.W.; Turnbull, G.A. Organic Semiconductor Lasers. *Chem. Rev.* **2007**, *107*, 1272–1295. [CrossRef]
5. Tessler, N. Lasers Based on Semiconducting Organic Materials. *Adv. Mater.* **1999**, *11*, 363–370. [CrossRef]
6. Jiang, Y.; Liu, Y.-Y.; Liu, X.; Lin, H.; Gao, K.; Lai, W.-Y.; Huang, W. Organic Solid-State Lasers: A Materials View and Future Development. *Chem. Soc. Rev.* **2020**, *49*, 5885–5944. [CrossRef]
7. Forget, S.; Chénais, S. *Organic Solid-State Lasers*; Springer: Berlin/Heidelberg, Germany, 2013; Volume 175, ISBN 978-3-642-36704-5.
8. Woggon, T.; Klinkhammer, S.; Lemmer, U. Compact Spectroscopy System Based on Tunable Organic Semi-conductor Lasers. *Appl. Phys. B* **2010**, *99*, 47–51. [CrossRef]
9. Clark, J.; Lanzani, G. Organic Photonics for Communications. *Nat. Photonics* **2010**, *4*, 438–446. [CrossRef]
10. Lu, M.; Choi, S.S.; Irfan, U.; Cunningham, B.T. Plastic Distributed Feedback Laser Biosensor. *Appl. Phys. Lett.* **2008**, *93*, 111113. [CrossRef]
11. Wang, Y.; Morawska, P.O.; Kanibolotsky, A.L.; Skabara, P.J.; Turnbull, G.A.; Samuel, I.D.W. LED Pumped Polymer Laser Sensor for Explosives. *Laser Photon Rev.* **2013**, *7*, L71–L76. [CrossRef]

12. Farrando-Pérez, Á.; Villalvilla, J.M.; Quintana, J.A.; Boj, P.G.; Díaz-García, M.A. Top-Layer Resonator Organic Distributed Feedback Laser for Label-Free Refractive Index Sensing. *Adv. Opt. Mater.* **2024**, *12*, 2401284. [CrossRef]
13. Vannahme, C.; Klinkhammer, S.; Christiansen, M.B.; Kolew, A.; Kristensen, A.; Lemmer, U.; Mappes, T. All-Polymer Organic Semiconductor Laser Chips: Parallel Fabrication and Encapsulation. *Opt. Express* **2010**, *18*, 24881. [CrossRef] [PubMed]
14. Vannahme, C.; Klinkhammer, S.; Kolew, A.; Jakobs, P.-J.; Guttmann, M.; Dehm, S.; Lemmer, U.; Mappes, T. Integration of Organic Semiconductor Lasers and Single-Mode Passive Waveguides into a PMMA Substrate. *Microelectron. Eng.* **2010**, *87*, 693–695. [CrossRef]
15. Shukla, A.; Mai, V.T.N.; Senevirathne, A.M.C.; Allison, I.; McGregor, S.K.M.; Lepage, R.J.; Wood, M.; Matsu-shima, T.; Moore, E.G.; Krenske, E.H.; et al. Low Amplified Spontaneous Emission and Lasing Thresholds from Hybrids of Fluorenes and Vinylphenylcarbazole. *Adv. Opt. Mater.* **2020**, *8*, 2000784. [CrossRef]
16. Tang, X.; Lee, Y.-T.; Feng, Z.; Ko, S.Y.; Wu, J.W.; Placide, V.; Ribierre, J.-C.; D'Aléo, A.; Adachi, C. Color-Tunable Low-Threshold Amplified Spontaneous Emission from Yellow to Near-Infrared (NIR) Based on Donor–Spacer–Acceptor–Spacer–Donor Linear Dyes. *ACS Mater. Lett.* **2020**, *2*, 1567–1574. [CrossRef]
17. Khan, A.; Tang, X.; Zhong, C.; Wang, Q.; Yang, S.; Kong, F.; Yuan, S.; Sandanayaka, A.S.D.; Adachi, C.; Jiang, Z.; et al. Intramolecular-Locked High Efficiency Ultrapure Violet-Blue (CIE-y < 0.046) Thermally Activated Delayed Fluorescence Emitters Exhibiting Amplified Spontaneous Emission. *Adv. Funct. Mater.* **2021**, *31*, 2009488. [CrossRef]
18. Shukla, A.; Wallwork, N.R.; Li, X.; Sobus, J.; Mai, V.T.N.; McGregor, S.K.M.; Chen, K.; Lepage, R.J.; Krenske, E.H.; Moore, E.G.; et al. Deep-Red Lasing and Amplified Spontaneous Emission from Nature Inspired Bay-Annulated Indigo Derivatives. *Adv. Opt. Mater.* **2020**, *8*, 1901350. [CrossRef]
19. Ribierre, J.-C.; Zhao, L.; Inoue, M.; Schwartz, P.-O.; Kim, J.-H.; Yoshida, K.; Sandanayaka, A.S.D.; Nakanotani, H.; Mager, L.; Méry, S.; et al. Low Threshold Amplified Spontaneous Emission and Ambipolar Charge Transport in Non-Volatile Liquid Fluorene Derivatives. *Chem. Commun.* **2016**, *52*, 3103–3106. [CrossRef]
20. Kim, H.; Schulte, N.; Zhou, G.; Müllen, K.; Laquai, F. A High Gain and High Charge Carrier Mobility Indeno-fluorene-Phenanthrene Copolymer for Light Amplification and Organic Lasing. *Adv. Mater.* **2011**, *23*, 894–897. [CrossRef]
21. Kanibolotsky, A.L.; Vilela, F.; Forgie, J.C.; Elmasly, S.E.T.; Skabara, P.J.; Zhang, K.; Tieke, B.; McGurk, J.; Belton, C.R.; Stavrinou, P.N.; et al. Well-Defined and Monodisperse Linear and Star-Shaped Quaterfluorene-DPP Molecules: The Significance of Conjugation and Dimensionality. *Adv. Mater.* **2011**, *23*, 2093–2097. [CrossRef]
22. Schneider, D.; Rabe, T.; Riedl, T.; Dobbertin, T.; Kröger, M.; Becker, E.; Johannes, H.-H.; Kowalsky, W.; Wei-mann, T.; Wang, J.; et al. Ultrawide Tuning Range in Doped Organic Solid-State Lasers. *Appl. Phys. Lett.* **2004**, *85*, 1886–1888. [CrossRef]
23. Nakanotani, H.; Furukawa, T.; Adachi, C. Light Amplification in an Organic Solid-State Film with the Aid of Triplet-to-Singlet Upconversion. *Adv. Opt. Mater.* **2015**, *3*, 1381–1388. [CrossRef]
24. Wallikewitz, B.H.; Hertel, D.; Meerholz, K. Cross-Linkable Polyspirobifluorenes: A Material Class Featuring Good OLED Performance and Low Amplified Spontaneous Emission Thresholds. *Chem. Mater.* **2009**, *21*, 2912–2919. [CrossRef]
25. Nakanotani, H.; Akiyama, S.; Ohnishi, D.; Moriwake, M.; Yahiro, M.; Yoshihara, T.; Tobita, S.; Adachi, C. Ex-tremely Low-Threshold Amplified Spontaneous Emission of 9,9′-Spirobifluorene Derivatives and Electrolu-minescence from Field-Effect Transistor Structure. *Adv. Funct. Mater.* **2007**, *17*, 2328–2335. [CrossRef]
26. Komino, T.; Nomura, H.; Yahiro, M.; Endo, K.; Adachi, C. Dependence of the Amplified Spontaneous Emission Threshold in Spirofluorene Thin Films on Molecular Orientation. *J. Phys. Chem. C* **2011**, *115*, 19890–19896. [CrossRef]
27. Han, Y.-M.; Sun, C.; Bai, L.-B.; Lin, J.-Y.; Xu, M.; Liu, Y.-Y.; Ding, X.-H.; Xie, L.-H.; Shen, K.; Qin, T.-S.; et al. Photoexcitation Dynamics of Thiophene–Fluorene Fluorophore in Matrix Encapsulation for Deep-Blue Am-plified Spontaneous Emission. *ACS Appl. Polym. Mater.* **2021**, *3*, 1306–1313. [CrossRef]
28. Han, Y.; Sun, C.; Bai, L.; Zuo, Z.; Xu, M.; Yu, M.; An, X.; Wei, C.; Lin, J.; Wang, N.; et al. Matrix Encapsulation of Solution-Processed Thiophene-Based Fluorophores for Enhanced Red and Green Amplified Spontaneous Emission. *Phys. Status Solidi (RRL) Rapid Res. Lett.* **2020**, *14*, 1900493. [CrossRef]
29. Zu, G.; Li, S.; He, J.; Zhang, H.; Fu, H. Amplified Spontaneous Emission from Organic Phosphorescence Emitters. *J. Phys. Chem. Lett.* **2022**, *13*, 5461–5467. [CrossRef]
30. Muñoz-Mármol, R.; Zink-Lorre, N.; Villalvilla, J.M.; Boj, P.G.; Quintana, J.A.; Vázquez, C.; Anderson, A.; Gordon, M.J.; Sastre-Santos, A.; Fernández-Lázaro, F.; et al. Influence of Blending Ratio and Polymer Matrix on the Lasing Properties of Perylenediimide Dyes. *J. Phys. Chem. C* **2018**, *122*, 24896–24906. [CrossRef]
31. Vembris, A.; Muzikante, I.; Karpicz, R.; Sliauzys, G.; Miasojedovas, A.; Jursenas, S.; Gulbinas, V. Fluorescence and Amplified Spontaneous Emission of Glass Forming Compounds Containing Styryl-4H-Pyran-4-Ylidene Fragment. *J. Lumin.* **2012**, *132*, 2421–2426. [CrossRef]
32. Popova, S.; Pudzs, K.; Latvels, J.; Vembris, A. Light Emitting and Electrical Properties of Pure Amorphous Thin Films of Organic Compounds Containing 2-Tert-Butyl-6-Methyl-4H-Pyran-4-Ylidene. *Opt. Mater.* **2013**, *36*, 529–534. [CrossRef]
33. Zarins, E.; Siltane, K.; Pervenecka, J.; Vembris, A.; Kokars, V. Glass-Forming Derivatives of 2-Cyano-2-(4H-Pyran-4-Ylidene) Acetate for Light-Amplification Systems. *Dye. Pigment.* **2019**, *163*, 62–70. [CrossRef]
34. Vembris, A.; Zarins, E.; Kokars, V. Stimulated Emission and Optical Properties of Pyranyliden Fragment Containing Compounds in PVK Matrix. *Opt. Laser Technol.* **2017**, *95*, 74–80. [CrossRef]
35. Reichardt, C. Solvatochromic Dyes as Solvent Polarity Indicators. *Chem. Rev.* **1994**, *94*, 2319–2358. [CrossRef]

36. Vembris, A.; Zarins, E.; Kokars, V. Solid State Solvation Effect and Reduced Amplified Spontaneous Emission Threshold Value of Glass Forming DCM Derivative in PMMA Films. *J. Lumin.* **2015**, *158*, 441–446. [CrossRef]
37. Bulović, V.; Shoustikov, A.; Baldo, M.A.; Bose, E.; Kozlov, V.G.; Thompson, M.E.; Forrest, S.R. Bright, Saturated, Red-to-Yellow Organic Light-Emitting Devices Based on Polarization-Induced Spectral Shifts. *Chem. Phys. Lett.* **1998**, *287*, 455–460. [CrossRef]
38. Bulović, V.; Deshpande, R.; Thompson, M.E.; Forrest, S.R. Tuning the Color Emission of Thin Film Molecular Organic Light Emitting Devices by the Solid State Solvation Effect. *Chem. Phys. Lett.* **1999**, *308*, 317–322. [CrossRef]
39. Deshpande, A.V.; Beidoun, A.; Penzkofer, A.; Wagenblast, G. Absorption and Emission Spectroscopic Inves-tigation of Cyanovinyldiethylaniline Dye Vapors. *Chem. Phys.* **1990**, *142*, 123–131. [CrossRef]
40. Anni, M. Poly [2-methoxy-5-(2-ethylhexyloxy)-1,4-phenylenevinylene] (MeH-PPV) Amplified Spontaneous Emission Optimization in Poly(9,9-dioctylfluorene (PFO):MeH-PPV Active Blends. *J. Lumin.* **2019**, *215*, 11668. [CrossRef]